nature geoscience

SUPPLEMENTARY INFORMATION

DOI: 10.1038/NGEO2181

Silica burial enhanced by iron limitation in oceanic upwelling margins

Pichevin L. E.[1], Ganeshram R. S.[1], Geibert W.[1], Thunell R.[2], Hinton R.[1]

1. School of Geosciences, Grant Institute, University of Edinburgh, West Main Road, EH9 3JW, Edinburgh, UK, laetitia.pichevin@ed.ac.uk, Tel +44 131 650 8547, Fax +44 131 668 3184

2. Dept. of Earth and Ocean Sciences, University of South Carolina, Columbia, SC 29208, USA

Supplementary material

1. Global compilation of biogenic silica fluxes and the Si:Corg ratio

Biogenic silica fluxes from the sea surface vary greatly between different parts of the ocean (Calvert 1966; Demaster 1981; Sirocko 1991; Tréguer, Nelson et al. 1995; Ragueneau, Treguer et al. 2000). In Figure S1 we show an ocean-wide compilation of normalised biogenic fluxes recorded in 140 sediment traps deployed within the framework of the US JGOFS endeavour (Thunell 1998aa; Honjo, Steven et al. 2008 and references therein). Areas of high Biogenic Silica (BioSi) fluxes (red) correspond to the Southern Ocean (SO), the North and Equatorial Pacific (NP and EP) and few upwelling continental margins. Export production in these areas is also characterised by high silica to organic carbon ratios ($Si:C_{org}$ > 1). While $Si:C_{org}$ and BioSi fluxes vary by 1 and 3 orders of magnitude respectively, amongst the sediment traps, inorganic and organic carbon fluxes and their ratios are relatively constant, suggesting that the variation in $Si:C_{org}$ ratio is mainly due to variations in the flux of BioSi rather than the relative contributions of calcareous and naked planktonic species to the

total production. It is worth mentioning that there is no relationship between the Si:C_{org} ratio and the trap depth.

We further evaluate whether the large changes in Si:C_{org} ratio in the settling particles (Fig1 in text) between basins can be explained by changes in siliceous versus calcareous production and the ballast efficiency of organic carbon by siliceous and calcareous skeletal remains. To do so, we use a modified version of the ballast model of Armstrong (Armstrong, Lee et al. 2002) whereby organic carbon fluxes can be accounted for by the fluxes of the other biogenic constituents (inorganic carbon and silica) multiplied by a "ballasting" coefficient (Armstrong, Lee et al. 2002). This coefficient describes the efficiency of a given inorganic constituent to transport organic carbon to depth and therefore quantifies the contribution of each inorganic fraction to the export of organic carbon. Our model varies from Armstrong et al (2002) and (Klaas and Archer 2002), in that the ballast factor not only describes the physical ability of the calcareous shells or siliceous frustules to carry organic matter through the water column but also depends on the original Cinorg:Corg and Si:Corg ratio of the producers. Although Armstrong et al (2002) also included the contribution of clay fluxes in their ballast model, we only consider BioSi and Cinorg fluxes here because clay fluxes are not always determined for the samples available. However, more than 90% of the Corg fluxes can be explained by the BioSi and C_{inorg} fluxes without including clay or free settling organic matter in the equation. Our ballast model is described by the following equation:

$$FCorg = \alpha \times FCinorg + \beta \times FSi, \qquad \text{(equation 1)}$$

Where FCorg is the modelled organic carbon flux, FCinorg is the recorded inorganic carbon flux, FSi is the recorded biogenic silica flux, α is the ballast factor of inorganic carbon and β is the ballast factor of biogenic silica.

Figure S2 shows the good agreement between data and modelled Corg for all the sediment traps. We found that the best fit between data and model occurs for different α and β factors depending on the trap location or ocean regime. For low Si flux areas such as the Atlantic and Indian Ocean, the best fit between data and modelled Corg fluxes was reached for $\alpha = 0.8$ and $\beta = 0.4$. Applying these values to high Si Fluxes sediment traps resulted in largely over estimating the Corg fluxes. For high Si flux regions such as the NP, the SO or the EP margins, where Si:Corg rain ratio > 1, the best fit between data and modelled Corg fluxes was reached for $\alpha = 1$ and $\beta = 0.1$ (Fig. S2, bottom).

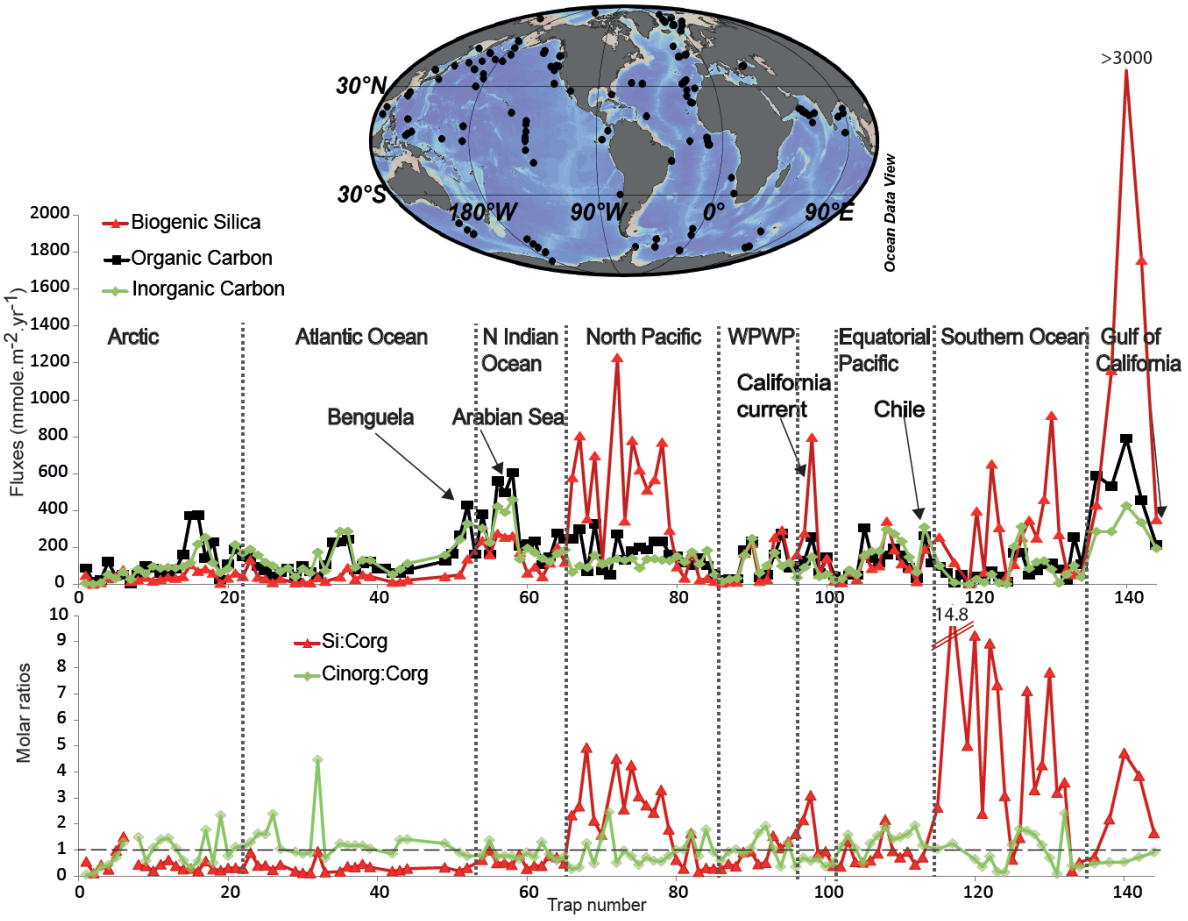

Figure S1: Ocean-wide compilation of normalised biogenic fluxes recorded in 140 sediment traps deployed within the framework of the US JGOFS endeavour (Thunell 1998a; Ragueneau, Treguer et al. 2000; Honjo, Steven et al. 2008 and references therein). The Gulf of California results correspond to mass fluxes recorded in the same sediment trap at

different times during the 7-year record period: summer, winter, El Nino, maximum upwelling conditions and El Niño conditions. The position of the sediment traps is shown on the map (top). Biogenic fluxes (middle) and molar ratios of the fluxes (bottom) are shown for each region considered. WPWP stands for Western Pacific Warm Pool. The fluxes have all been corrected for water depth (Honjo, Steven et al. 2008).

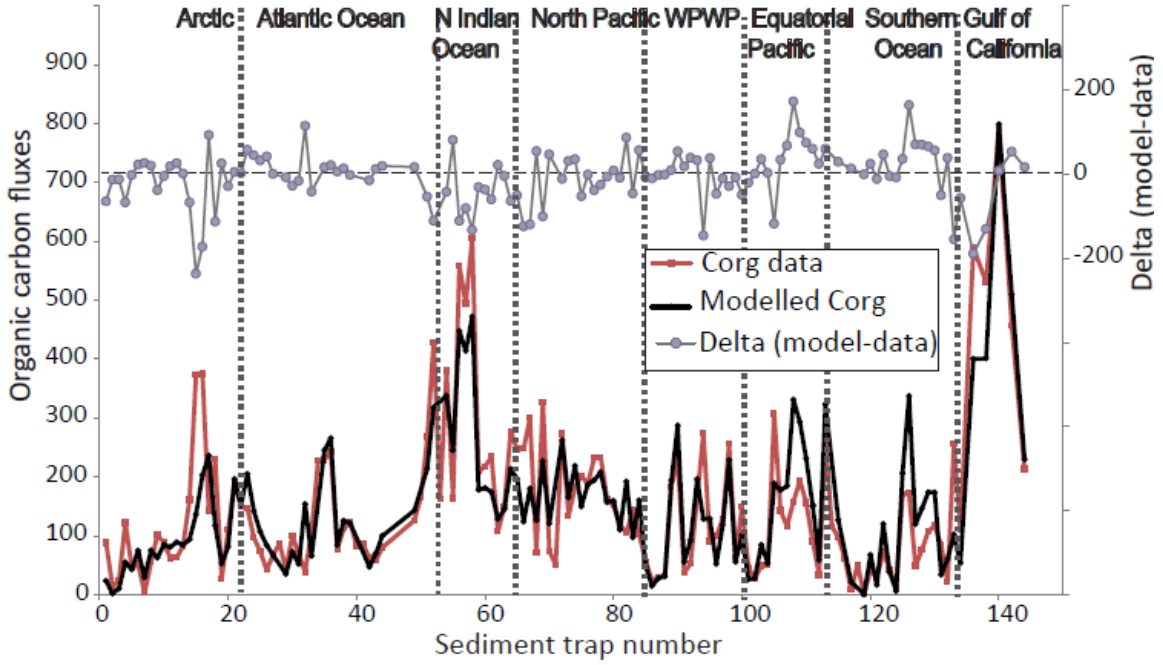

Modelled Corg fluxes : FCorg = α x FCinorg + β x FSi

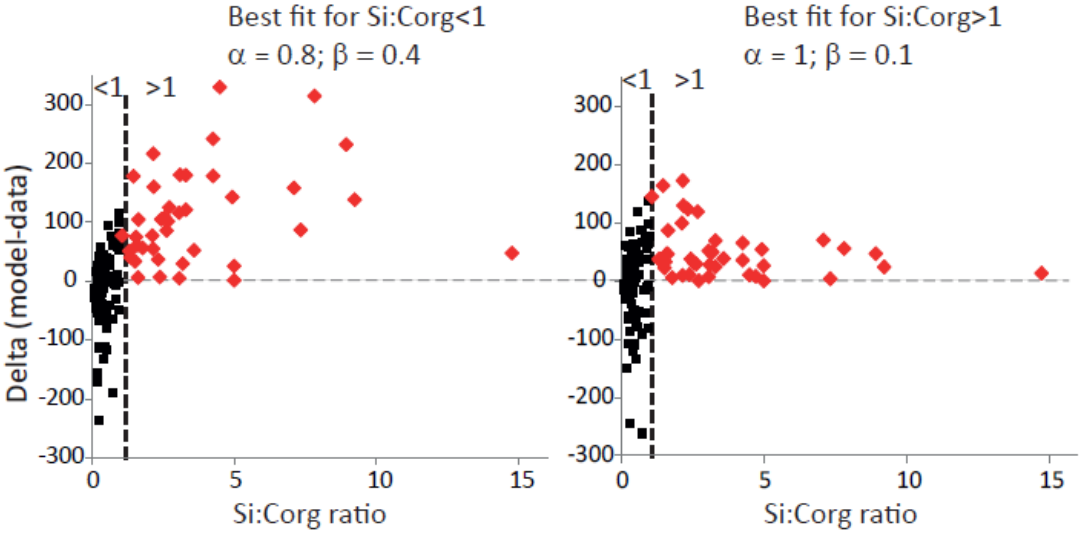

Figure S2: *(Top) Comparison between organic carbon fluxes recorded in the traps and modelled from the fluxes of other biogenic constituents following equation 1. Grey dashed lines represent the limit between the different oceanic provinces considered, similar to Figure S1. The delta (model-data) represents the difference between the recorded and modelled organic carbon fluxes. The best fit between data and model occurs for different ballast coefficients (α and β) depending on the Si:Corg ratio in the sediment trap. For Si:Corg ratio <1, α = 0.8 and β = 0.4. while α = 1 and β = 0.1 when the Si:Corg ratio in the traps is >1.*

As the photosynthesis to calcification (molar Corg:Cinorg) ratio in a coccolithophore bloom is generally equal to or slightly less than 1 (Robertson, Robinson et al. 1994), the values we find for α in both cases (1 and 0.8) appears reasonable and indicates the carbon transported by the calcareous plankton is well preserved during settling. However, the molar Corg:Si ratio in diatoms is 3.5 +/- 1 on average (Brzezinski 1985; Hutchins and Bruland 1998), while we calculate ballast factors (β) of between 0.1 and 0.4 for biogenic silica. This indicates lower export efficiency for the organic carbon carried by diatom frustules and other siliceous plankton compared to carbonates. Moreover, the decrease from 0.4 to 0.1 in the export factor of biogenic silica (β) in the traps characterised by high BioSi fluxes (Si:Corg > 1) implies that either the ballasting effect of biogenic silica (mainly diatom frustules) is further reduced in these environments relative to the rest of the ocean or that the Si:C ratio of the settling diatoms is greater in these regions. The former is implausible as evidence shows that preservation rates of BioSi and Corg in the SO for instance are not different from the rest of the ocean (Pondaven, Ragueneau et al. 2000; Ragueneau, Dittert et al. 2002). On the other hand, in high nutrient-low chlorophyll regions such as the SO, the NP and the equatorial Pacific, Fe limitation results in an average 3 fold increase in the uptake of Si relative to C by diatoms. Therefore, we propose that the reduction from 0.4 to 0.1 in the ballast coefficient of

bioSi in areas characterised by high BioSi fluxes and Si:Corg ratios is largely due to the increase in the Si:Corg ratio of the diatoms growing under conditions of Fe limitation. Similarly in upwelling margins such as the California current region and the GoC, high Si fluxes during upwelling are due to higher nutrient uptake ratio by diatoms similar to the SO and other HNLC regions. After accounting for species change and the ballasting effect the model requires Si:C uptake ratios by diatoms to be several times (up to 4.5) greater during upwelling seasons compared to non-upwelling seasons in the GoC (Fig. 2, c). It is worth noting that the eastern Pacific sediment trap data presented here represent annual averages and therefore the expected seasonal increase in the Si:Corg ratio with the development of Fe limitation during intense upwelling is not captured in Figure S1. Further analysis of the Santa Barbara basin sediment trap time series (Thunell 1998b) indeed reveals that there is a 3 fold increase in the Si:Corg export ratio (1.4 from 0.4) during the upwelling season relative to the stratified period indicative of the effect of Fe limitation on the diatoms in this basin, similar to our observations in the GoC (http://usjgofs.whoi.edu/mzweb/data/Honjo/sed_traps.html #Pacific). Similar seasonal changes in the Si:Corg ratio of the biological production with upwelling intensity is also observed in the Cariaco Basin (Thunell, Benitez-Nelson et al. 2008).

2. Revised Global Marine Si Budget

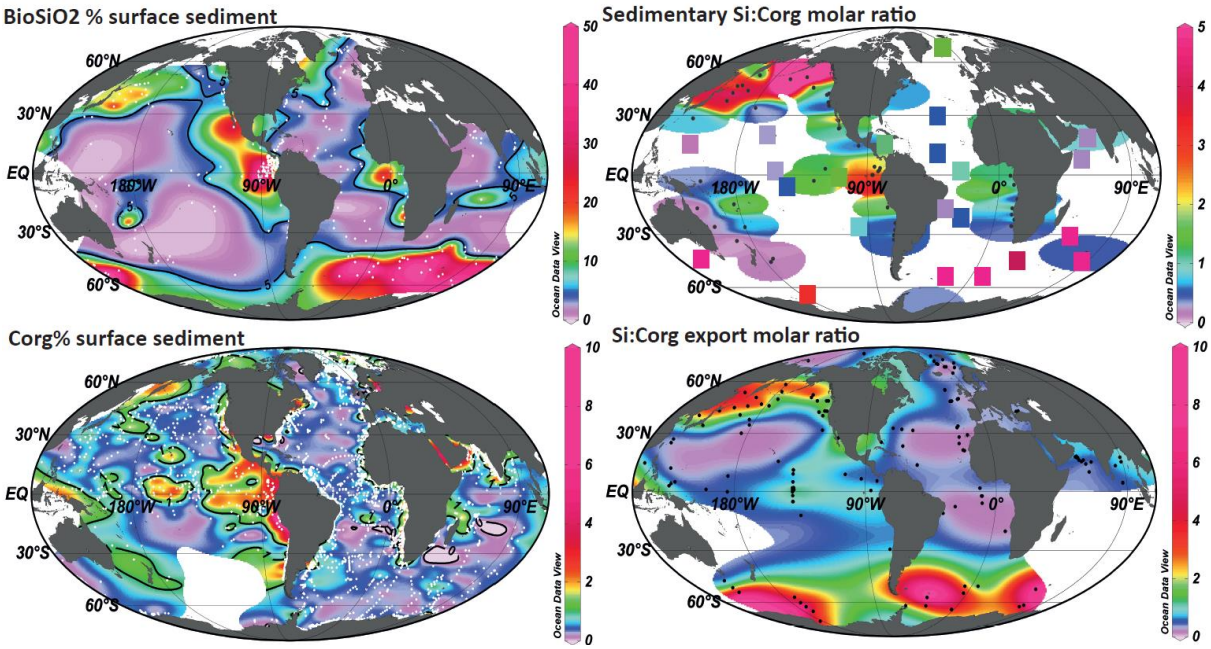

Figure S3: (Left) Distribution of organic carbon (Corg) and biogenic silica (wt. %) in surface sediments (SINOPS data compilation http://www. pangaea.de/PangaVista?query=sinops, (Heinze, Hupe et al. 2003; Seiter, Hensen et al. 2004 and Pichevin unpublished) and (right) calculated burial Si:Corg molar ratio in the surface sediment compared to that in sediment traps (Ragueneau, Treguer et al. 2000; Honjo, Steven et al. 2008). Coloured squares on the top right panel represent estimates of the Si:C molar ratio averaged from several core top data when both Corg and BioSi % were not available in the same core. White and black dots represent core top and trap locations. Core top data are available at Pangaea.de

In Figure S3 we show that core top Si:Corg ratios are variable (ranging from 0.4 to 1.2) and to a large extent follow sediment trap export ratios (Ragueneau, Treguer et al. 2000; Honjo, Steven et al. 2008). This provides the basis to refine existing biogenic silica burial fluxes in the ocean where Si burial fluxes were estimated from Corg fluxes using a constant ratios of 0.6 (DeMaster 2002; Tréguer and De La Rocha 2013), For instance, Si:Corg export ratio of

0.9 to 5 is observed in the sediment traps from the north-eastern tropical Pacific margin (Fig.S1 and S). If particulate Si:Corg is transferred to the sediments and buried at such elevated ratios, then the current marine Si budgets probably underestimate the margin Si sink. Using a compilation of core top organic carbon and biogenic silica data (Heinze, Hupe et al. 2003; Seiter, Hensen et al. 2004) we were able to estimate the $Si:C_{org}$ molar ratio in 64 core tops globally distributed and to estimate the $Si:C_{org}$ ratio in a further 21 areas where both Corg and BioSi were not available at the same site (Fig. S3).

The distribution of the core top $Si:C_{org}$ ratio shows a very good agreement with that of the export $Si:C_{org}$ ratio from the sediment trap data set indicating in general that water column top $Si:C_{org}$ signal is transferred to the sediments (Fig. S3). The exception are the equatorial west African margin and the coastal EEP where the sedimentary $Si:C_{org}$ burial ratios are higher than expected from the water column export ratios. This mismatch is likely due to the lack of sediment trap data directly adjacent to the West African and EEP coasts (values extrapolated from trap data farther off shore). The SO and NP show the highest Si:Corg burial ratio (2 to >10), followed by the EEP (1.5 to 4). Amongst the continental margin sites or domain, the Eastern Tropical North Pacific (ETNP) shows the highest $Si:C_{org}$ (0.6-4). These areas represent the main Si burial hotspot (see BioSi% map, Fig. S3). The Arabian Sea has a very low $Si:C_{org}$ burial ratio as predicted by the export fluxes. This core-top compilation confirms that Fe limitation in areas such as the SO, NP, the EEP and ETNP enhances sedimentary Si burial by increasing the $Si:C_{org}$ ratio of the growing diatoms. The $Si:C_{org}$ burial ratio at margin sites (average slope is 0.98) and the Si:Corg burial ratios in the ETNP (from 0.6 to 3) estimated from our more comprehensive compilation, is much higher than the Si:Corg ratio of 0.6 (0.4-1.2) used in previous marine Si inventories (DeMaster 2002; Tréguer and De La Rocha 2013). In addition, areas with high $Si:C_{org}$ burial ratios are also characterised by the highest organic carbon and bulk mass accumulation rates in the whole

ocean (Berger, Smetacek et al. 1989). Using published Corg burial rates (Berger, Smetacek et al. 1989) and sedimentary Si:Corg ratios specific to each margin (this study, Fig. S3), we estimate that the Si sink in coastal zones could be as high as 3.7+/-1.1 Tmol $Si.yr^{-1}$ with enhanced Si sink located in the coastal EEP and ETNP where we suggest Fe limitation occurs.

In summary, our compilation and records from the ETNP lead to a revision of the existing Si budgets (Table 1). We suggests that about ¾ of the Si sink may occur in margins and open ocean HNLC regions, such as the SO, NP, GoC, California Current, Equatorial Pacific (Si:Corg ratio > 1, Fig. S1), where Si burial is enhanced by Fe limitation, Indeed the ETNP is estimated to be the largest margin sink (up to 50% of the total margin sink).

Regions	**Mean biogenic Si accumulation rates** mmole $SiO_2.m^{-2}.yr^{-1}$	**Surface area** $10^{12}m^{-2}$	**Silicon sink** Tmole $SiO_2.yr^{-1}$	**References**	**Fe limitation?**
Eastern Tropical North Pacific	1500 (100-10000)	1	1.5	Estimate based on a, c, d	Yes, Transient
Eastern Tropical South Pacific	<360	1.1	<0.4	Estimate based on a	Needs further study
Entire Arabian Sea	10 (5-25)	3.8	0.038	Estimate based on b	No Evidence
Other Margins			1.8	This study	Not applicable
Margins (total)			3.7	This study	At least 45%, Transient
Southern ocean			2	Treguer et al, 2013	Yes
Open Ocean			1.04	Treguer et al, 2013	Yes, 50-70% (N & Equatorial Pacific)
Total			6.7	Treguer et al, 2013; This study	60% to 75%

Table 1: Estimates of Si accumulation and burial rates in the sediments of the main upwelling-influenced continental margins (light grey) and recent marine Si budget (Treguer et al., 2013, dark grey) highlighting the influence of Fe limitation on the distribution and intensity of Si sedimentary burial in the ocean. The silicon sinks were estimated by

multiplying the surface area by average biogenic silica accumulation rates (a) Demaster 1981; b) Sirocko 1991; c) Arellano-Torres, Pichevin et al. 2011; d) Pichevin, Ganeshram et al. 2012). This table illustrates that biogenic Si accumulation rates are 2 to 3 orders of magnitude) higher in the North eastern Pacific relative to the Arabian Sea upwelling areas. The eastern Pacific margin locations collectively represent the greatest Si sink despite covering smaller area than the Arabian Sea for instance.

3. Methodology: Diatom-bound trace metal analyses

3.1 Selection of samples and preparation of the diatom concentrates for trace element analysis

The trap samples used in this study were collected between March 1996 and February 1997 during a long-term trap deployement from August 1990 in the Guaymas Basin (27º53'N, 111º40'W, Fig. S6 of the supplementary material) (Thunell 1998a). The samples were collected continuously for 2 weeks using an automated sediment trap situated 500 m below the sea surface and 200 m above the sea floor. Sampling details are published in (Thunell 1998a).

Calypso Core MD-02 2515 was retrieved from the Guaymas Basin (27°29.01N; 112°04.46W; 881m water depth) during the MONA (Marges Ouest Nord Américaines) cruise of the R/V Marion Dufresne (International Marine Global Changes-IMAGES VIII) in June 2002. The core is well dated with an age model based on 28 AMS ^{14}C assays of organic matter. The age model has been published recently in (McClymont, Ganeshram et al. 2012; Pichevin, Ganeshram et al. 2012).

The suspended particulate Weddell Gyre samples were collected during cruise ANT XX/2 of FS "Polarstern" in December/January 2002/2003 (Geibert, Assmy et al. 2010). For each sample, particulate matter was extracted from several hundred litres of sea water using a large-volume continuous flow centrifuge with a trace-element clean sample introduction system (Schussler and Kremling 1993). Samples were freeze-dried on board and subsequently cleaned as described below.

Purification of the diatom samples for trace metal measurement was performed following published cleaning methods (Ellwood and Hunter 1999; Morley, Leng et al. 2004; Hendry and Rickaby 2008). The procedure includes both mechanical and chemical cleaning steps. Approximately 0.5 to 1g of sediment was subsampled into a 50ml centrifuge tube and

carbonates and organic matter were removed using 5% HCl and 40% H_2O_2, respectively, prior to further separation of the diatoms from clays and other terrigenous components. The mechanical step consists of elimination of large debris by sieving (at 10 and 75 microns), differential settling using a heavy liquid (density set at 2.1g/ml) as well as screening of the sample under the microscope to verify the purity of the diatom fraction (Morley, Leng et al. 2004). The chemical cleaning includes 3 steps and is performed on the isolated diatom fraction to ensure the absence of terrigenous contamination on the diatom frustules. The reagents used for the cleaning process were 1% hydroxylamine chloride in acetic acid; 0.1% w/w NaF solution and 50% strong-acid solution of ultrapure HNO_3 and HCl as described in (Hendry and Rickaby 2008). Potential contamination was subsequently tested using the ion microprobe (see below).

3.2 Trace-metal measurements in the diatom frustules

The trace metal measurements on cleaned diatom frustules were performed on an Ion Microprobe Cameca ims-4f at the NERC (National Environment Research Council) Microprobe Facility located at the School of Geosciences , University of Edinburgh. The Ion Microprobe employs Secondary Ion Mass Spectrometry (SIMS) for the chemical analysis of small volumes of material for most isotopes in the periodic table. With destructive conventional methods (ICP-MS & OES) it is difficult to guarantee that all the terrigenous material has been successfully eliminated at the surface of the frustules. Unlike ICP-MS/OES techniques which involve dissolution of the sample, the Ion Microprobe method enables us to differentiate between the terrigenous coatings potentially remaining on the frustules surface from the biologically-fixed metals inside the siliceous matrix. This allows for more accurate measurements of diatom-bound metals while bypassing the need to use more aggressive cleaning methods. It is also theoretically possible to determine if exchange processes during early diagenesis in marine sediments affect the trace metal signal of the frustules. The clean diatom samples (2 mg) were pressed into an indium foil and analysed several (10-12) times for up to 10 cycles with the ion microprobe. We used a 10nA primary beam, 25 micron image field and energy filtering (75eV). The metal:SiO_2 values on the plots (Fig. 1 and 2 of the paper and Fig. S4) represent the average of the 10-12 measurements made for each sample. Each measurement focussed on a single or a couple of isolated diatom frustules, therefore it was important to analyse several diatoms in each sample in order to account for 1) the variability in the sample and 2) obtain realistic and statistically significant average values (Fig. S4a).

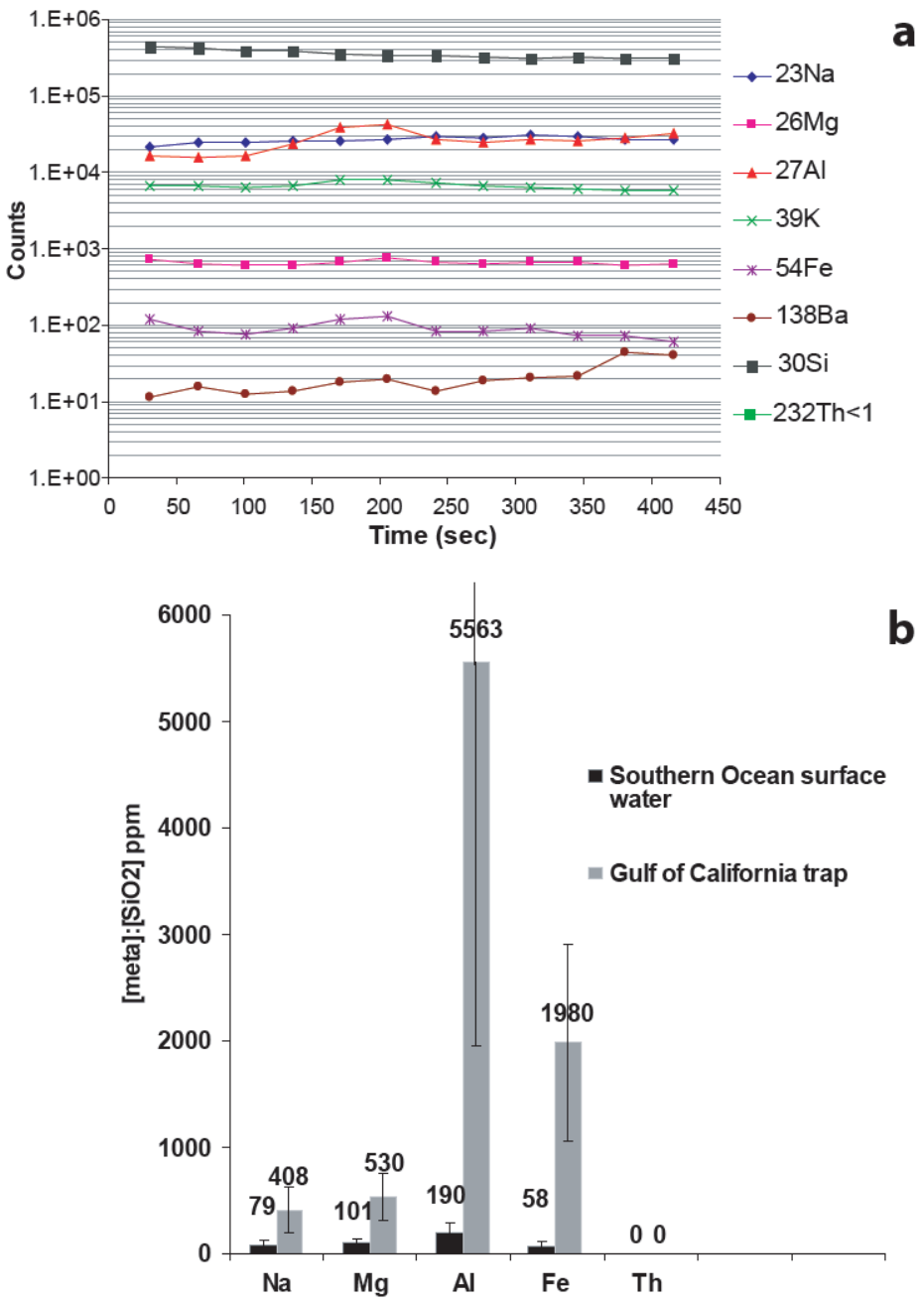

Figure S4: ***(a)*** *Typical 25 microns pin-point SIMS analysis of a diatom from Core MD-02 2515 showing the stability of the atomic counts for each metal throughout the analyses as the ion beam "digs" through the frustule. This particular analysis consisted in 12 cycles of measurements lasting 7 minutes in total. This approach allows determining spatial variations in the metal concentration within the frustules as well as any surface contamination.* ***(b)*** *Metal (Na, Mg, Al, Fe, Th) to SiO_2 ratios measured in modern diatoms collected from the*

Weddell Sea surface waters (black) and the Gulf of California sediment traps (grey) using the ion microprobe technique.

The following isotopes were measured in both trap and sedimentary diatom samples as well as in Weddell Gyre surface diatom samples and in a standard for comparison: ^{23}Na, ^{26}Mg, ^{27}Al, ^{30}Si, ^{54}Fe, ^{232}Th. Potential terrigenous (clay) contamination and signs of early diagenesis were assessed by measuring ^{232}Th and ^{27}Al in the diatoms frustules, respectively. Contamination or diagenetic incorporation of metals would result in relatively high levels of Th or Al at the surface of the frustules during the first couple of measurement cycles, rapidly decreasing as the ion beam penetrates inside the opal matrix. This trend was never observed in our samples which all showed very constant metal levels throughout the analyses demonstrating the cleanliness of the diatom frustules and that the metal contents determined were associated with the matrix of the frustules (Fig. S4a). Moreover, the element/Al ratios measured in the frustules are different from the upper crustal values hence further ruling out terrigenous contamination.

Metal concentrations in the diatom frustules from the Guaymas Basin trap are shown in Figure S4b. Thorium (^{232}Th) levels are undetectable in the diatoms, showing the absence of terrigenous contamination. This is confirmed by the stability of metal signal during each pin-point ion Microprobe analysis as the beam penetrates the cleaned diatom frustules and indicates that the elements are homogeneously incorporated within the opal matrix and not present as surface contaminants. Apart from Si, Al is the most abundant metal in the diatom frustules with average levels of 5563ppm (5.56‰) in the Guaymas Basin samples. These concentrations are very comparable to those found in coastal diatoms studied by (Hendry and Rickaby 2008). However, Al is much less abundant in the diatoms from the Weddle gyre. Dissolved Al has a short residence time in the ocean and is expected to be much more

concentrated in coastal environments that receive terrigenous inputs than in the open ocean like the Weddell Sea. Therefore the 50-fold difference in Al:SiO_2 levels between both locations is interpreted as reflecting the disparity in dissolved Al concentration between the studied regions. Diatom-bound Mg and Na concentrations are one order of magnitude lower than diatom-bound Al and Fe concentrations while dissolved Na and Mg concentrations in sea water are on average 6 to 7 orders of magnitude higher than marine Al concentration and about 8 orders of magnitude higher than dissolved Fe concentration (Broecker and Peng 1984). Therefore, there is an elemental enrichment in Al and Fe relative to Mg and Na in the frustules. Aluminium has been shown to be structurally associated with silicon in the opal matrix both when the organisms synthesise their frustules and post deposition during diagenesis (Dixit, Van Cappellen et al. 2001; Gehlen, Beck et al. 2002). Because our samples are suspended or settling diatoms, we expect the diagenetic inclusion of Al to be negligible and incorporation during synthesis potentially explains the high Al concentrations compared to Mg and Na in the diatoms from the Guaymas basin. The relatively high Fe concentration in the frustules compared to Mg and Na also indicates that there is selective incorporation of Fe (enrichment) in the frustules while Mg and Na are probably more “passively” incorporated into the frustules (Lal, Charles et al. 2006). This is not surprising as Fe is an essential nutrient for diatom growth and therefore more biologically reactive than Mg and Na.

3.3 Relationship between diatom-bound Fe and dissolved Fe concentrations in sea water

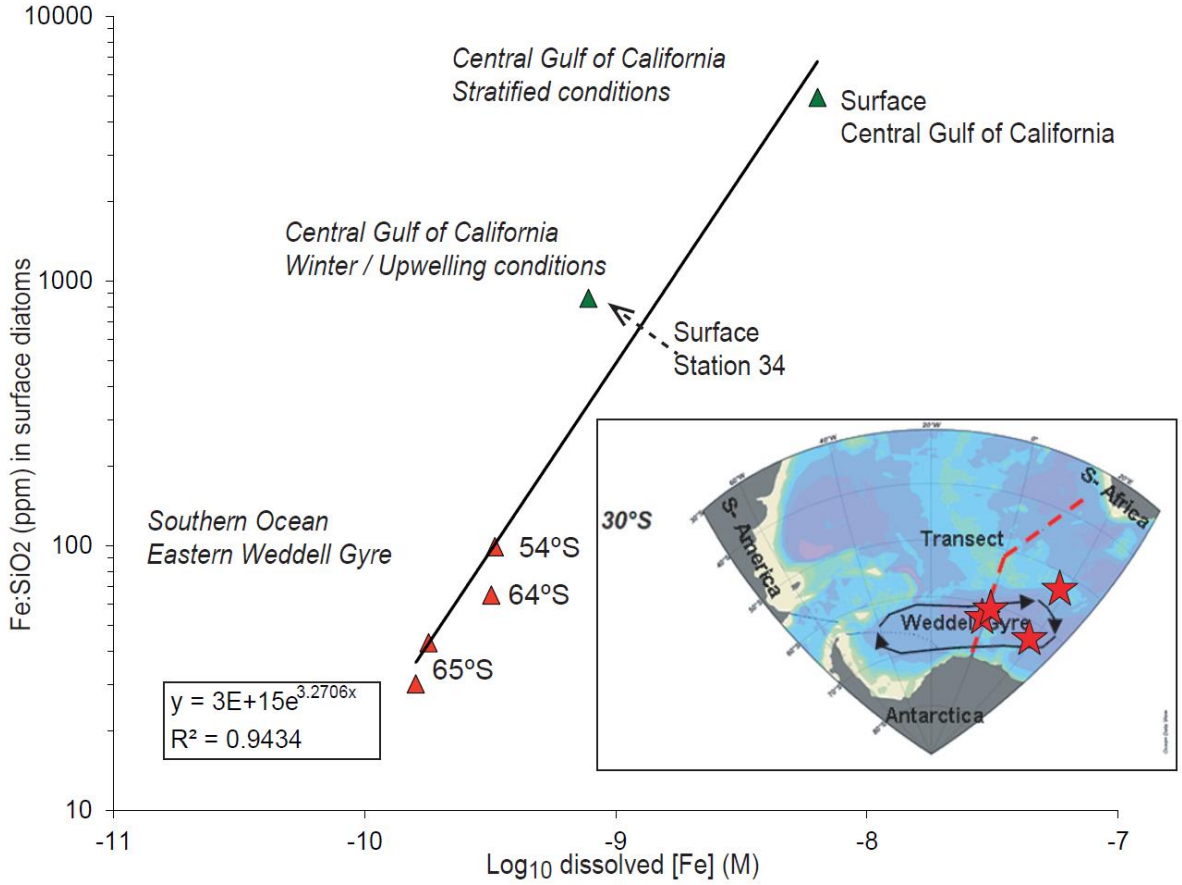

Figure S5: Dissolved iron concentration (as log10) measured in the surface water of the Weddell Gyre (red triangles, cruise track is marked by the red line on the map) and the Gulf of California (green triangles) (Segovia-Zavala, Lares et al. 2010; Klunder, Laan et al. 2011) plotted against Molar Fe:Si ratio (ppm) measured in diatom frustules collected in the same regions (red stars on the map) and during similar conditions (upwelling, stratified condition). Surface dFe data from the central Gulf of California represent stratified condition with high Fe concentration at the sea surface due to terrigenous inputs while surface dFe data from station 34 represent conditions at the end of the upwelling season when nutrients are depleted due to biological utilisation. The Fe:Si ratio in the frustules increases with increasing Fe concentration in the photic zone.

Comparison of diatom-bound trace metal concentrations between the Guaymas Basin trap samples and the surface diatoms from the southern Ocean (Weddell Sea) is shown in Figure S5b. The SO receives between 50 and 100 times less dust than the Gulf of California (Jickells, An et al. 2005; Mahowald, Engelstaedter et al. 2009). Al and Fe concentrations in the diatom frustules from the Guaymas basin trap are around 30-50 times greater than in the diatoms from the Weddell Sea potentially reflecting the sharp contrast in micronutrient availability between these two areas. Diatom-bound Mg and Na concentration however remain fairly comparable between both regions which could be explained by the facts that Mg and Na behave as conservative elements in the ocean.

A finer comparison between both areas is shown for Fe. In Figure S5, Fe:SiO_2 ratios in diatoms from the surface of the SO (East of the Weddell Gyre) and the GoC are plotted against dissolved Fe (dFe) concentrations measured recently in the same locations by (Segovia-Zavala, Lares et al. 2010; Klunder, Laan et al. 2011). We specifically compared the diatom-bound Fe values we obtained for each area with dFe concentrations measured in nearby locations and in similar conditions. For instance the average July-August Fe/SiO_2 value is plotted against the dFe concentration measured in stratified condition in the GoC near the sediment trap site while the average winter Fe:SiO_2 value is plotted against dFe concentration recorded in upwelling condition (Segovia-Zavala, Lares et al. 2010). Similarly, diatom-bound Fe values from the WS are plotted against dFe concentrations from nearby sites (Fig. 5) (Klunder, Laan et al. 2011). Although we are aware both data sets (diatom-bound and dissolved metal concentrations) were not determined in exactly the same location or at the same time and both spatial and temporal variations can be expected in dissolved iron concentrations, our comparison clearly shows that greater dFe concentrations are correlated with higher Fe/SiO_2 ratios in the diatoms. Stratified conditions in the GoC result in about 8 times higher dissolved Fe concentrations at the sea surface compared to upwelling conditions

(Segovia-Zavala, Lares et al. 2010). Similarly, diatoms sampled during stratified conditions contain about 6 times more Fe in their frustules (standardised over SiO_2) than diatoms collected during upwelling/winter conditions when Fe availability decreases due to biological utilisation. Similarly, in the WS, dFe concentration is 3 times higher at 54°S compared to 65°S which results in 3 fold higher Fe/SiO_2 in diatoms from 54°S compared to 65°S. We observe a linear relationship between dissolved Fe concentrations in the surface ocean and Fe/SiO_2 ratios in diatoms sampled in corresponding environment/conditions suggesting that diatoms incorporate metals in their hard part in proportion to the availability of these metals in the ambient seawater (Ellwood and Hunter 1999; Ellwood and Hunter 2000; Lal, Charles et al. 2006; Hendry and Rickaby 2008; Jaccard, Ariztegui et al. 2009; Jaccard, Ariztegui et al. 2009). While such relationship has been shown in laboratory experiments for Zn, the data set presented here is the first comparison in natural conditions furnishing strong support for the use of diatom-bound metal concentrations as tracers for micronutrient availability. In addition, our data further suggests that the incorporation of Fe in the diatoms hard parts is not strongly species dependent as different assemblages of diatoms are expected to live in environments as different as the SO the GoC. The wide range of Fe concentrations considered in this particular study is comparable to the range of dissolved Fe observed in the whole ocean today from Fe-limiting to Fe-replete conditions. These initial results showing a linear relationship between Fe biological availability and diatom-bound Fe suggests the potential for this application in other oceanic regions with further in situ work in order to refine the calibration.

4. Transient iron limitation and Si burial in the Gulf of California (GoC)

4.1 Iron deficit and Si utilisation in the GoC

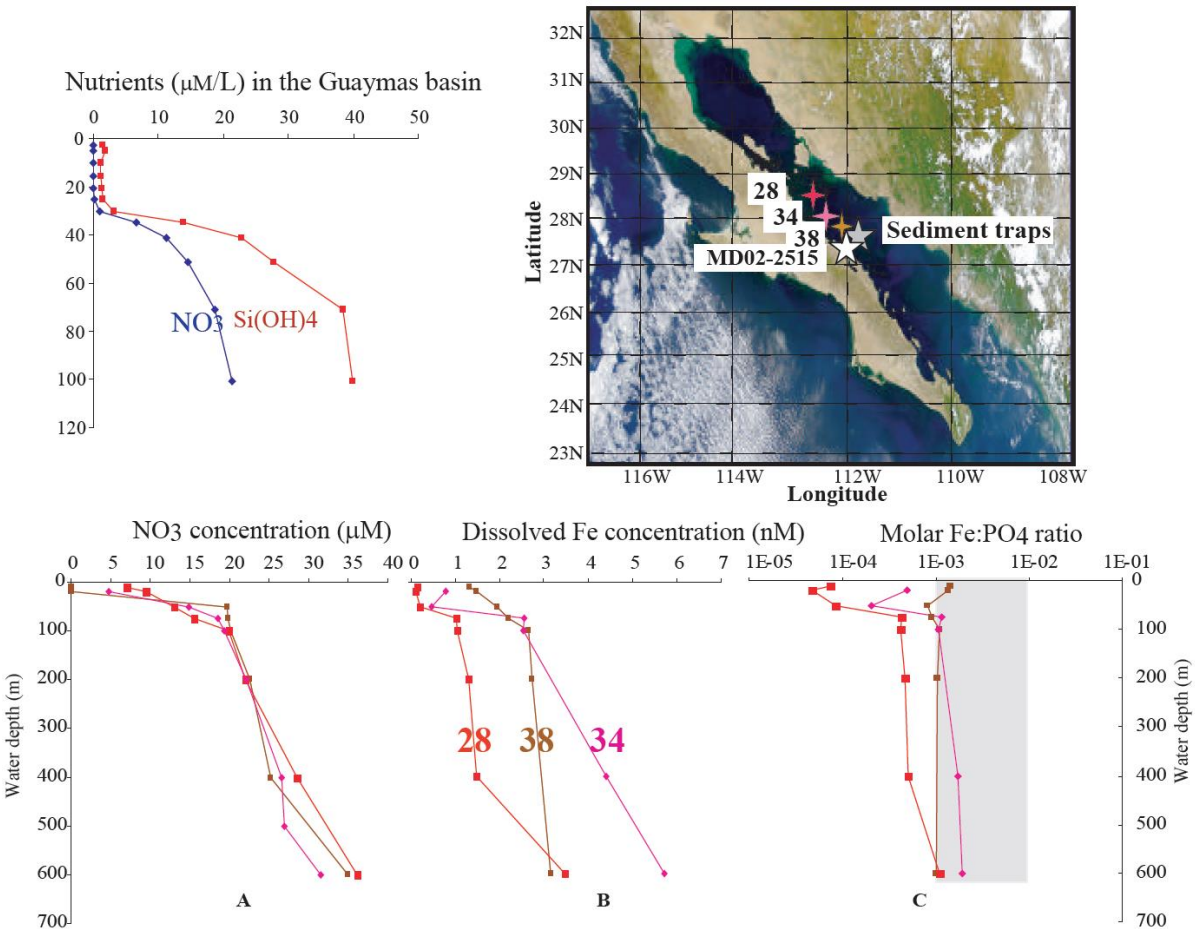

Figure S6: Map of the Gulf of California showing the locations of sediment core MD 02-2515 (white star), the sediment trap (grey star) and the water stations 24 (red), 34 (pink) and 38 (brown) from (Segovia-Zavala, Lares et al. 2010) (top right). Depth profile of silicic acid and nitrate in the Guaymas basin (top left), nitrate, and dissolved iron concentrations and the PO_4:Fe ratio at stations 24, 34 and 38 (Segovia-Zavala, Lares et al. 2010). The light grey shading highlights the range of optimum subsistence Fe:PO_4 ratio for marine organisms below which Fe becomes limiting for growth. Note that this ratio is probably higher for coastal diatoms (Twining, Baines et al. 2011) (bottom).

Macronutrients and dissolved iron (dFe) distributions in the central region of the GoC (just north of the Guaymas Basin) were measured in spring 2003 (Segovia-Zavala, Lares et al. 2010). Locations of the stations and nutrient profiles are shown in Figure S6 of the supplementary material, respectively. Both PO_4 and dFe exhibit typical nutrient profiles with relatively high concentrations at depth (3 μM and 1-5 nM, respectively) and low concentrations at the surface (1-1.5 μM and 0.1-1 nM, respectively) due to biological consumption in the top 100 meters of the water column (Segovia-Zavala, Lares et al. 2010). Nitrate concentration in the water column follows the same trend (not shown). The molar ratio of dFe to PO_4 was calculated from *Segovia-Zavala et al.* [2010] data and shown in firure 1.c. The dFe:PO_4 ratio is generally close to or below 10^{-3} with the exception of the surface water at 27.8ºN (closest to Guaymas Basin) and at depth at 28.1ºN where the molar ratio reaches about $1.5x10^{-3}$ (Fig. S6). Eucaryotic plankton in coastal areas have a subsistence optimum Fe:PO_4 ratio of between 10^{-2} and $10^{-3.1}$ although studies show that there are important variations between phytoplankton types (Brand 1991 and references there in). A recent study in the Equatorial Pacific suggests that diatoms have up to 6 times greater Fe requirements than other phytoplankton groups such as coccoliths and flagellates (Twining, Baines et al. 2011) and display Fe:PO_4 molar ratios close to $6x10^{-3}$ (compared to 10^{-3} for other groups). Therefore, the dFe:PO_4 ratio in the GoC in the vicinity of the Guaymas Basin is generally well below the optimum subsistence ratio for coastal diatoms and close to the limit for other phytoplankton groups. Considering the dominance of diatoms relative to other phytoplankton groups in the GoC, this deficit should lead to Fe limitation if other continental and shelf Fe sources are not able to compensate during periods of high biological productivity (Firme, Rue et al. 2003; Fitzwater, Johnson et al. 2003). This creates a strong propensity for the development of transient iron limitation during intense upwelling at the surface of the GoC.

In Figure S6, modern nutrient profiles reveal that silicic acid in subsurface waters is in excess relative to nitrate. Pichevin et al. (2012) reported that SiO_2 is incompletely utilised during winter upwelling events. Based on trap and nutrient data, this study suggested that the depletion of silicic acid is related to elevated biological utilisation of silicic acid relative to nitrate during/following intense upwelling episodes, most probably due to the occurrence of transient iron limitation. Given that the SiO_2 to NO_3- ratio of 1.8 in upwelling waters (SiO2 in excess of diatoms growth at optimum conditions) this study predicted that dampened upwelling and the lifting of Fe limitation should lead to presence of excess silicic acid in the surface waters. Downcore record $\delta^{30}Si$ from the GoC confirms this prediction highlighting the impact of the occurrence of transient Fe limitation on Si utilisation and burial (below).

4.2 Multiproxy reconstruction of silica cycling and iron biological availability in the GoC over the last climatic cycle in core MD 02-2515

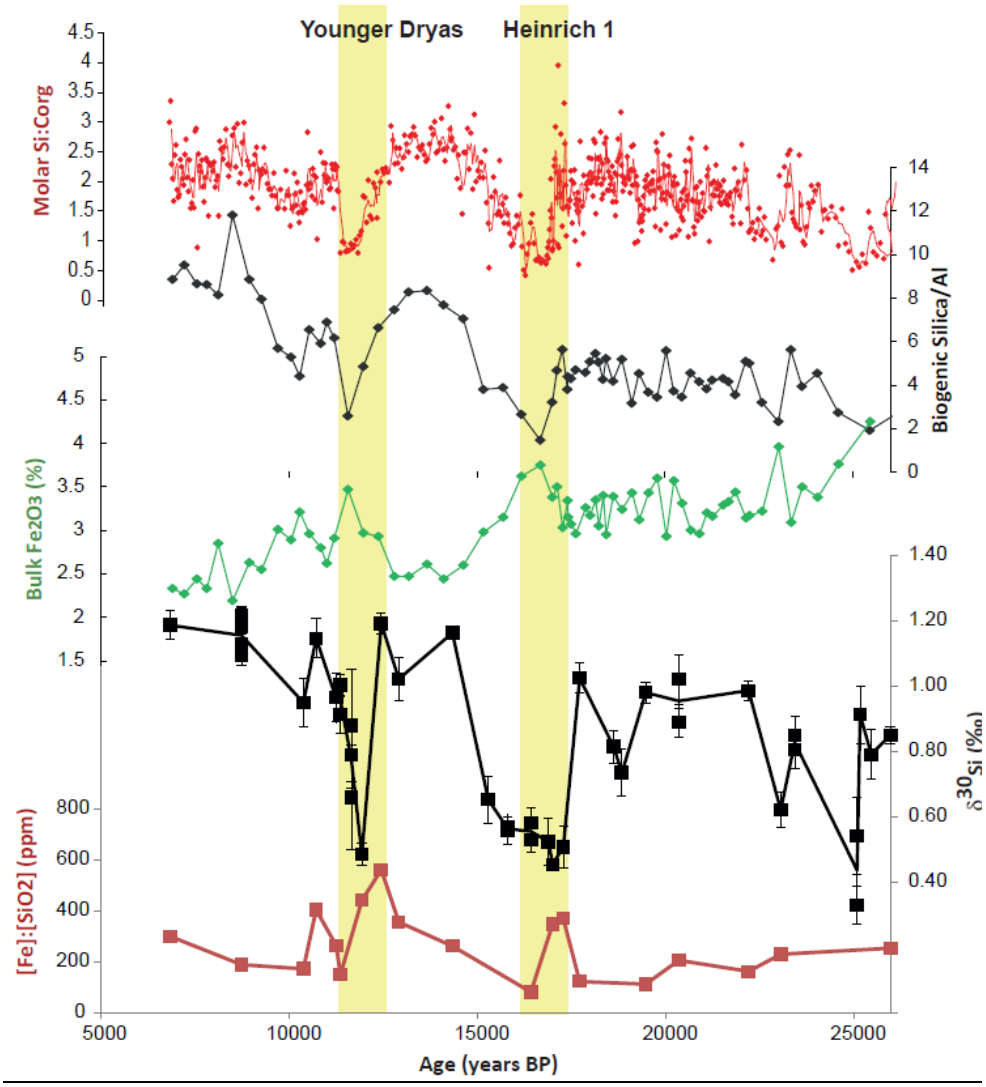

*Figure S7: (bottom to top) Fe:SiO2 ratios (ppm) measured in sedimentary diatoms (**a**) compared with silicic acid utilisation (δ^{30}Si ‰, Pichevin et al., 2012, **b**), bulk (%, **c**), biogenic silica accumulation (Si/Al, **(d)** and molar silicon to organic carbon (Si:Corg) ratio **(e)** from Core MD 02-2515. Yellow stripes highlight cold climatic periods corresponding to the Younger Dryas and Heinrich event 1 as identified in Greenland ice cores. These periods of increased diatom-bound Fe concentration and decreasing biogenic silica export to the sediment are generally associated with lower silicic acid utilisation at the sea surface.*

High-resolution sedimentary records from Core MD022515 in the GoC are shown in Fig 6 of the supplementary material. Due to shallow water depth at the core site, aluminium normalisation is used rather than the more refined ^{230}Th normalisation technique to evaluate biogenic silica accumulation (Francois, Frank et al. 2004). Variations in diatom-bound Fe:SiO2 ratios are not reflected in terrigenous fluxes, demonstrating that biological availability of Fe is not related to the supply of continental inputs but to the biological consumption of Fe in the surface water.

The δ^{30}Si varies between 0.45‰ and 1.2‰ with higher values occurring during the Holocene and Bølling-Allerød (B/A). The most striking feature of this record is the low values documented during the YD, H1 and H2. The δ^{30}Si record seems to parallel BioSi % with low δ^{30}Si when BioSi accumulation is low in the Guaymas Basin. The δ^{30}Si values of dissolved silicic acid supplied to the GoC are estimated to be around 1.2‰ (De la Rocha, Brzezinski et al. 2000; Reynolds, Frank et al. 2006). During the mid-early Holocene and the B/A, the δ^{30}Si signal in Core MD 02-2515 is ~1.2‰. Therefore, this value approximates the isotopic signature of the modern silicic acid source. This suggests that the relative utilisation of silicic acid was nearly complete during these time intervals. Using a Raleigh fractionation model (equation 1 below) in a closed system, we find that relative silicic acid utilisation during Heinrich events was about 50%. Considering the subsurface Silicic acid to nitrate ratio of about 1.8, we would expect that in the absence of Fe limitation, the diatoms would consume silicic acid and nitrate with a 1:1 ratio until all the nitrates are consumed, leaving about 50% (44%) of the silicic acid unutilised. Therefore, the δ^{30}Si values measured during Heinrich events are consistent with the absence of Fe limitation at that time while the δ^{30}Si values measured during the Holocene are consistent with complete utilisation of Silicic acid under conditions of Fe limitation.

(Equation 1) $$[\delta^{30}\mathrm{Si}_{\mathrm{diatoms}}]_f = [\delta^{30}\mathrm{Si}_{\mathrm{silica}}]_{f=1} + [\alpha \ln(f) \times f/(1-f)]$$

Where, F is the fraction of unutilised silicic acid, α is the fractionation factor (about 1), $\delta^{30}\mathrm{Si}_{\mathrm{silica}}$ is 1.2 ‰ and $\delta^{30}\mathrm{Si}_{\mathrm{diatoms}}$ is the accumulated product (0.5‰ during Heinrich events).

References

Arellano-Torres, E., L. E. Pichevin, et al. (2011). "High-resolution opal records from the eastern tropical Pacific provide evidence for silicic acid leakage from HNLC regions during glacial periods." Quaternary Science Reviews **30**(9-10): 1112-1121.

Armstrong, R. A., C. Lee, et al. (2002). "A new, mechanistic model for organic carbon fluxes in the ocean based on the quantitative association of POC with ballast minerals." Deep-Sea Research Part Ii-Topical Studies in Oceanography **49**(1-3): 219-236.

Berger, W., V. Smetacek, et al. (1989). Ocean productivity and paleoproductivity: an overview. In Productivity of the Ocean: Present and Past. V. S. WH Berger, G Wefer. New York, Wiley**:** 1–34.

Brand, L. E. (1991). "Minimum Iron Requirements of Marine-Phytoplankton and the Implications for the Biogeochemical Control of New Production." Limnology and Oceanography **36**(8): 1756-1771.

Broecker, W. S. and T. H. Peng (1984). Tracers in the Sea. New York, Eldigio Press.

Brzezinski, M. A. (1985). "The Si-C-N Ratio of Marine Diatoms - Interspecific Variability and the Effect of Some Environmental Variables." Journal of Phycology **21**(3): 347-357.

Calvert, S. E. (1966). "Origin of Diatom-Rich Varved Sediments from Gulf of California." Journal of Geology **74**(5P1): 546-&.

De la Rocha, C. L., M. A. Brzezinski, et al. (2000). "A first look at the distribution of the stable isotopes of silicon in natural waters." Geochimica Et Cosmochimica Acta **64**(14): 2467-2477.

Demaster, D. J. (1981). "THE SUPPLY AND ACCUMULATION OF SILICA IN THE MARINE-ENVIRONMENT." Geochimica Et Cosmochimica Acta **45**(10): 1715-1732.

DeMaster, D. J. (2002). "The accumulation and cycling of biogenic silica in the Southern Ocean: revisiting the marine silica budget." Deep-Sea Research Part Ii-Topical Studies in Oceanography **49**(16): 3155-3167.

Dixit, S., P. Van Cappellen, et al. (2001). "Processes controlling solubility of biogenic silica and pore water build-up of silicic acid in marine sediments." Marine Chemistry **73**(3-4): 333-352.

Ellwood, M. J. and K. A. Hunter (1999). "Determination of the Zn/Si ratio in diatom opal: a method for the separation, cleaning and dissolution of diatoms." Marine Chemistry **66**(3-4): 149-160.

Ellwood, M. J. and K. A. Hunter (2000). "The incorporation of zinc and iron into the frustule of the marine diatom Thalassiosira pseudonana." Limnology and Oceanography **45**(7): 1517-1524.

Firme, G. F., E. L. Rue, et al. (2003). "Spatial and temporal variability in phytoplankton iron limitation along the California coast and consequences for Si, N, and C biogeochemistry." Global Biogeochemical Cycles **17**(1).

Fitzwater, S. E., K. S. Johnson, et al. (2003). "Iron, nutrient and phytoplankton biomass relationships in upwelled waters of the California coastal system." Continental Shelf Research **23**(16): 1523-1544.

Francois, R., M. Frank, et al. (2004). "Th-230 normalization: An essential tool for interpreting sedimentary fluxes during the late Quaternary." Paleoceanography **19**(1).

Gehlen, M., L. Beck, et al. (2002). "Unraveling the atomic structure of biogenic silica: Evidence of the structural association of Al and Si in diatom frustules." Geochimica Et Cosmochimica Acta **66**(9): 1601-1609.
Geibert, W., P. Assmy, et al. (2010). "High productivity in an ice melting hot spot at the eastern boundary of the Weddell Gyre." Global Biogeochemical Cycles **24**.
Heinze, C., A. Hupe, et al. (2003). "Sensitivity of the marine biospheric Si cycle for biogeochemical parameter variations." Global Biogeochemical Cycles **17**(3).
Hendry, K. R. and R. E. M. Rickaby (2008). "Opal (Zn/Si) ratios as a nearshore geochemical proxy in coastal Antarctica." Paleoceanography **23**(2).
Honjo, S., J. M. Steven, et al. (2008). "Particulate organic carbon fluxes to the ocean interior and factors controlling the biological pump: A synthesis of global sediment trap programs since 1983." Progress in Oceanography **76**.
Hutchins, D. A. and K. W. Bruland (1998). "Iron-limited diatom growth and Si : N uptake ratios in a coastal upwelling regime." Nature **393**(6685): 561-564.
Jaccard, T., D. Ariztegui, et al. (2009). "Assessing past changes in bioavailable zinc from a terrestrial (Zn/Si)(opal) record." Chemical Geology **258**(3-4): 362-367.
Jaccard, T., D. Ariztegui, et al. (2009). "Incorporation of zinc into the frustule of the freshwater diatom Stephanodiscus hantzschii." Chemical Geology **265**(3-4): 381-386.
Jickells, T. D., Z. S. An, et al. (2005). "Global iron connections between desert dust, ocean biogeochemistry, and climate." Science **308**(5718): 67-71.
Klaas, C. and D. E. Archer (2002). "Association of sinking organic matter with various types of mineral ballast in the deep sea: Implications for the rain ratio." Global Biogeochemical Cycles **16**(4).
Klunder, M. B., P. Laan, et al. (2011). "Dissolved iron in the Southern Ocean (Atlantic sector)." Deep-Sea Research Part Ii-Topical Studies in Oceanography **58**(25-26): 2678-2694.
Lal, D., C. Charles, et al. (2006). "Paleo-ocean chemistry records in marine opal: Implications for fluxes of trace elements, cosmogenic nuclides (Be-10 and Al-26), and biological productivity." Geochimica Et Cosmochimica Acta **70**(13): 3275-3289.
Mahowald, N. M., S. Engelstaedter, et al. (2009). "Atmospheric Iron Deposition: Global Distribution, Variability, and Human Perturbations." Annual Review of Marine Science **1**: 245-278.
McClymont, E. L., R. S. Ganeshram, et al. (2012). "Sea-surface temperature records of Termination 1 in the Gulf of California: Challenges for seasonal and interannual analogues of tropical Pacific climate change." Paleoceanography **27**.
Morley, D. W., M. J. Leng, et al. (2004). "Cleaning of lake sediment samples for diatom oxygen isotope analysis." Journal of Paleolimnology **31**(3): 391-401.
Pichevin, L., R. S. Ganeshram, et al. (2012). "Silicic acid biogeochemistry in the Gulf of California: Insights from sedimentary Si isotopes." Paleoceanography **27**.
Pondaven, P., O. Ragueneau, et al. (2000). "Resolving the 'opal paradox' in the Southern Ocean." Nature **405**(6783): 168-172.
Ragueneau, O., N. Dittert, et al. (2002). "Si/C decoupling in the world ocean: is the Southern Ocean different?" Deep-Sea Research Part Ii-Topical Studies in Oceanography **49**(16): 3127-3154.
Ragueneau, O., P. Treguer, et al. (2000). "A review of the Si cycle in the modem ocean: recent progress and missing gaps in the application of biogenic opal as a paleoproductivity proxy." Global and Planetary Change **26**(4): 317-365.
Reynolds, B. C., M. Frank, et al. (2006). "Silicon isotope fractionation during nutrient utilization in the North Pacific." Earth and Planetary Science Letters **244**(1-2): 431-443.

Robertson, J. E., C. Robinson, et al. (1994). "THE IMPACT OF A COCCOLITHOPHORE BLOOM ON OCEANIC CARBON UPTAKE IN THE NORTHEAST ATLANTIC DURING SUMMER 1991." Deep-Sea Research Part I-Oceanographic Research Papers **41**(2): 297-&.

Schussler, U. and K. Kremling (1993). "A PUMPING SYSTEM FOR UNDERWAY SAMPLING OF DISSOLVED AND PARTICULATE TRACE-ELEMENTS IN NEAR-SURFACE WATERS." Deep-Sea Research Part I-Oceanographic Research Papers **40**(2): 257-266.

Segovia-Zavala, J. A., M. L. Lares, et al. (2010). "Dissolved iron distributions in the central region of the Gulf of California, Mexico." Deep-Sea Research Part I-Oceanographic Research Papers **57**(1): 53-64.

Seiter, K., C. Hensen, et al. (2004). "Organic carbon content in surface sediments - defining regional provinces." Deep-Sea Research Part I-Oceanographic Research Papers **51**(12): 2001-2026.

Sirocko, F. (1991). "DEEP-SEA SEDIMENTS OF THE ARABIAN SEA - A PALEOCLIMATIC RECORD OF THE SOUTHWEST-ASIAN SUMMER MONSOON." Geologische Rundschau **80**(3): 557-566.

Thunell, R., C. Benitez-Nelson, et al. (2008). "Si cycle in the Cariaco Basin, Venezuela: Seasonal variability in silicate availability and the Si : C : N composition of sinking particles." Global Biogeochemical Cycles **22**(4).

Thunell, R. C. (1998a). "Seasonal and annual variability in particle fluxes in the Gulf of California: A response to climate forcing." Deep-Sea Research Part I-Oceanographic Research Papers **45**(12): 2059-2083.

Thunell, R. C. (1998b). "Particle fluxes in a coastal upwelling zone: sediment trap results from Santa Barbara Basin, California." Deep-Sea Research Part Ii-Topical Studies in Oceanography **45**(8-9): 1863-1884.

Tréguer, P. and C. De La Rocha (2013). "The world ocean silica cycle." Annual Review of Marine Science **5**: 477-501.

Tréguer, P., D. Nelson, et al. (1995). "The silica balance in the world ocean: a reestimate." Science (New York, N.Y.) **268**(5209): 375-379.

Twining, B. S., S. B. Baines, et al. (2011). "Metal quotas of plankton in the equatorial Pacific Ocean." Deep-Sea Research Part Ii-Topical Studies in Oceanography **58**(3-4): 325-341.